

21 Feb 2016

Application Of Generalized Snoek's Law Over A Finite Frequency Range: A Case Study

Konstantin N. Rozanov

Missouri University of Science and Technolgoy, rozanovk@mst.edu

Marina Y. Koledintseva

Missouri University of Science and Technology, marinak@mst.edu

Follow this and additional works at: https://scholarsmine.mst.edu/ele_comeng_facwork



Part of the [Electrical and Computer Engineering Commons](#)

Recommended Citation

K. N. Rozanov and M. Y. Koledintseva, "Application Of Generalized Snoek's Law Over A Finite Frequency Range: A Case Study," *Journal of Applied Physics*, vol. 119, no. 7, article no. 73901, American Institute of Physics, Feb 2016.

The definitive version is available at <https://doi.org/10.1063/1.4941844>

This Article - Journal is brought to you for free and open access by Scholars' Mine. It has been accepted for inclusion in Electrical and Computer Engineering Faculty Research & Creative Works by an authorized administrator of Scholars' Mine. This work is protected by U. S. Copyright Law. Unauthorized use including reproduction for redistribution requires the permission of the copyright holder. For more information, please contact scholarsmine@mst.edu.

RESEARCH ARTICLE | FEBRUARY 16 2016

Application of generalized Snoek's law over a finite frequency range: A case study

Konstantin N. Rozanov; Marina Y. Koledintseva

 Check for updates

J. Appl. Phys. 119, 073901 (2016)

<https://doi.org/10.1063/1.4941844>

 CHORUS



View Online



Export Citation

CrossMark

Articles You May Be Interested In

Extending the Snoek's limit of single layer film in (Co 96 Zr 4 / Cu) n multilayers

Appl. Phys. Lett. (October 2008)

Microwave permeability of Co 2 Z composites

J. Appl. Phys. (December 2004)

Eddy current effect on the microwave permeability of Fe-based nanocrystalline flakes with different sizes

J. Appl. Phys. (April 2014)

500 kHz or 8.5 GHz?
And all the ranges in between.

Lock-in Amplifiers for your periodic signal measurements



Find out more

 Zurich Instruments

Application of generalized Snoek's law over a finite frequency range: A case study

Konstantin N. Rozanov¹ and Marina Y. Koledintseva²

¹*Institute for Theoretical and Applied Electromagnetics, Moscow, Russia*

²*Oracle Corp., Menlo Park, California 94025, USA*

(Received 2 December 2015; accepted 1 February 2016; published online 16 February 2016)

Generalized Snoek's law proposed in an integral form by Acher and coauthors is a useful tool for investigation of high-frequency properties of magnetic materials. This integral law referred to as Acher's law allows for evaluating the ultimate performance of RF and microwave devices which employ magnetic materials. It may also be helpful in obtaining useful information on the structure and morphology of the materials. The key factor in practical application of Acher's law is an opportunity to employ either measured or calculated data available over a finite frequency range. The paper uses simple calculations to check the applicability of Acher's law in cases when the frequency range is limited and the magnetic loss peak is comparatively wide and has a distorted shape. The cases of large magnetic damping, pronounced skin effect, and inhomogeneity of the material are considered. It is shown that in most cases calculation of the integral through fitting of actual magnetic frequency dispersion by the Lorentzian dispersion law results in accurate estimations of the ultimate high-frequency performance of magnetic materials. © 2016 AIP Publishing LLC. [<http://dx.doi.org/10.1063/1.4941844>]

I. INTRODUCTION

Magnetic materials with high values of high-frequency permeability $\mu(f) = \mu'(f) - i\mu''(f)$, where f is the frequency, are important for various RF and microwave engineering applications (see Ref. 1 and references therein). The high-frequency permeability of a material can be evaluated based on the frequency of its ferromagnetic resonance (FMR), f_{res} , and the static permeability, μ_s . The value of f_{res} determines the frequency, above which the material is basically non-magnetic. The value of μ_s is an estimate of the permeability at lower frequencies. To have the dynamic permeability high, both μ_s and f_{res} should be high as well. For the majority of materials, the product of these values is limited according to Snoek's law²

$$(\mu_s - 1)f_{\text{res}} = \frac{2}{3}\gamma 4\pi M_0, \quad (1)$$

where $4\pi M_0$ is the saturation magnetization and $\gamma \approx 3 \text{ GHz/kOe}$ is the gyromagnetic ratio.

Equation (1) limits the achievable values of the high-frequency permeability. The materials, in which Snoek's limit is exceeded, are therefore of great interest. Equation (1) is rewritten for these materials as

$$(\mu_s - 1) \cdot f_{\text{res}}^2 \leq (\gamma 4\pi M_0)^2. \quad (2)$$

The limiting high-frequency magnetic properties correspond to the equality in (2) and are predicted in uniformly magnetized materials with the planar anisotropy, provided that two of three demagnetization factors are much less than the third one. The most important examples of such materials are thin ferromagnetic films,³ composites with flake-shaped magnetic inclusions,⁴ hexagonal ferrites,^{5,6} and some kinds of amorphous ferromagnetic microwires.⁷ In other materials, the left-hand side of (2) is smaller than the right-hand side, and

the high-frequency magnetic properties are well below the limiting value.

In inhomogeneous materials, inequality (2) is held provided that its right-hand side is multiplied by the concentration p of the magnetic phase in the material and by the spatial randomization factor κ . The latter takes into account the orientational distribution of magnetic moments and equals to the fraction of magnetic moments lying in the easy magnetic plane and perpendicular to the high-frequency magnetic field. Even though both factors p and κ are less than one, it is readily seen that Eq. (2) results in a significantly less stringent limitation than (1) for ferromagnetic materials in the microwave frequency range.

Limitations (1) and (2) are critical for modeling and optimization of microwave parameters of devices that use magnetic materials. For example, these conditions have been applied to determine the ultimate bandwidth of magnetic radar absorbers, since their operating frequency range is limited by the permeability values.⁸ Another example is the evaluation of the ultimate bandwidth of a patch antenna with a magnetic substrate.⁹ Equations (1) and (2) are useful for checking the correctness of the measured data and the results of numerical modeling of magnetic properties of materials.¹⁰ References 11–14 suggest the use of Eq. (2) for the analysis of magnetic structure of materials. The idea is based on the fact that a deviation from equality in (2) indicates a distortion of the magnetic structure in a ferromagnetic film or in platelets comprising a magnetic composite. In the films, a part of magnetic moments may rise out of the film plane due to the perpendicular magnetic anisotropy. In magnetic composites, the deviation may be because of the agglomeration of magnetic particles, porosity, or the presence of impurities.

Application of Eq. (2) is straightforward only for the simplest cases of frequency dispersion of permeability, e.g., when magnetic dissipation is low and magnetic loss has a

single narrow peak. It is also applicable when the magnetic loss peak is split due to the regular domain structure.^{10,15} However, Eq. (2) does not allow for obtaining any additional information in these cases as compared to the curve fitting of the measured permeability by the Landau-Lifshitz equation, which is the standard approach to analyze the microwave permeability.^{16–19}

The measured frequency dependences of magnetic loss often have wide peaks, which result from either inhomogeneity of materials or the presence of skin effect. In the case of wide loss peak, it is difficult to determine f_{res} , and Eq. (2) is not helpful any more. To evaluate microwave magnetic properties in this case, an integral analogue of (2) has been proposed²⁰

$$\frac{2}{\pi} \int_0^{\infty} \mu''(f) f df = (\gamma 4\pi M_0)^2. \quad (3)$$

Below, Eq. (3) is referred to as “integral Acher’s law” and the value in the left-hand side of (3) as “Acher’s constant,” K_A . Similar to (2), the right-hand side of (3) may contain the additional factor (κp) , which will be further omitted for the sake of simplicity.

For experimental validation of (3), the integral in the left-hand side of (3) is calculated^{10,21–24} using the measured frequency dependences of imaginary permeability. The upper limit of the integration equals to the highest measured frequency, f_{max} , and the integral is frequently normalized to the right-hand side of (3), i.e., the value of K_A

$$i_A(f_{\text{max}}) = \frac{1}{K_A} \frac{2}{\pi} \int_0^{f_{\text{max}}} \mu''(s) s ds. \quad (4)$$

The value of Acher’s constant is obtained from magneto-static measurements. It is seen from (3) and (4) that $i_A(f) \rightarrow 1$ at $f \rightarrow \infty$. The deviation of the results from the unity indicates the specifics of the material magnetic structure.

Equation (3) is derived from the Lorentzian law for frequency dispersion of permeability

$$\mu(f) = 1 + \frac{\mu_s - 1}{1 + if/f_{\text{rel}} - (f/f_{\text{res}})^2}, \quad (5)$$

where f_{rel} is the relaxation frequency. Dispersion law (5) follows from the Landau-Lifshitz equation with the Bloch-Bloembergen damping term, which does not provide for the conservation of magnetic moment during its precession. Therefore, even though the Lorentzian dispersion law is frequently used to describe the frequency dispersion in ferromagnetic materials,^{25–28} more rigorous approach is to use the dissipation term in Gilbert’s form, which yields the Landau-Lifshitz-Gilbert (LLG) frequency dependence of permeability

$$\mu(f) = 1 + \frac{4\pi\gamma M_0(f_y + i\alpha f)}{(f_x + i\alpha f)(f_y + i\alpha f) - f^2}, \quad (6)$$

where $f_x = \gamma(H_k + 4\pi M_0(N_x - N_z))$ and $f_y = \gamma(H_k + 4\pi M_0(N_y - N_z))$; H_k is the magnetic anisotropy field; N_x, N_y , and N_z are demagnetization factors of a single-domain ellipsoidal

particle along its three main axes; and α is the Gilbert dissipation parameter. In (6), the high-frequency magnetic field is assumed to be along the x axis, and the intrinsic magnetic moment of the particle is along the z axis. For the LLG dispersion (6), the equality in (2) is held when $f_y \gg f_x$ and $\alpha \ll 1$. If f_y and f_x are close to each other ($f_y \sim f_x$), then Snoek’s law (1) is valid.

Dispersion law (6) differs from (5) by the presence of an additional term proportional to the frequency in the numerator. It is known²⁹ that the integral in the right-hand side of (3) diverges if the frequency dependence of permeability obeys Eq. (6). From the standpoint of Eq. (4) that is used for estimating Acher’s integral for the data in a limited frequency range, the right part of the equation might exceed the unity if f_{max} is high enough. However, this has never been reported in the literature. It is commonly believed that the reason is a slow convergence of integral (4) at high dissipation. On the other hand, the slow convergence of the integral prevents from observing the “saturation,” or an asymptotic approaching of Acher’s integral $i_A(f)$ to a constant value as frequency increases, at least within the frequency range up to 20 GHz, where most of the reliable permeability measurements have been obtained. Therefore, the application of the integral formulation (4) does not allow for concluding about the magnetic structure of a material either.

When comparatively wide peaks of the measured magnetic loss are observed, they are frequently fitted by a series of Lorentzian terms^{30–32}

$$\mu(f) = \mu_{\infty} + \sum_j^n \frac{4\pi\chi_{s,j}}{1 + if/f_{\text{rel},j} - (f/f_{\text{res},j})^2}, \quad (7)$$

where $\chi_{s,j}$ is the static magnetic susceptibility of j -th resonance, n is the number of the resonances that is typically two or three, and μ_{∞} is the optical permeability that may be less than the unity in conducting magnetic materials because of the skin effect (see below). Alternatively, frequency dispersion of permeability may be described by a mixed frequency dependence that contains the same series as (7), but the term associated with FMR is in the LLG form (6), while the rest are the pure Lorentzian terms. Using the LLG term in such formulation frequently yields high values of the damping factor α , up to several hundreds.³³ On the other hand, it is known that damping in magnetic materials is due to a combination of intrinsic and extrinsic effects. The intrinsic effects are associated with the relaxation of magnetic moment at its precession. The extrinsic damping is mainly related to inhomogeneity of the material.³⁴ The intrinsic damping is characterized by $\alpha < 0.1$.³⁵ Higher values of α should therefore correspond to the extrinsic damping processes, i.e., to a distribution of resonant frequencies in different spatial regions of material. Then this distribution determines the shape of the loss peak, which could be different from both LLG and Lorentzian dispersion laws.

The feasibility of describing actual dispersion characteristics by the Lorentzian terms is crucial for the optimization of material magnetic properties for engineering applications, as well as for numerical electromagnetic modeling of materials and structures containing them, especially in the time

domain.³⁶ Equation (6) is substantially less convenient for such optimization, because it contains four parameters, while (5) contains only three parameters. The three principal characteristics of a loss peak are the magnitude, the position on the frequency axis, and the width. The fourth parameter describes asymmetry of the peak that may depend on many factors, including the material inhomogeneity. Therefore, the permeability fitting may result in a large uncertainty in this fourth parameter, and hence in the other three parameters, too. For this reason, when describing the permeability using the LLG frequency dispersion law, some additional assumptions are usually made, for example, $f_x = f_y$.^{11,33,37} Note that the main goal of using (7) is to get as accurate description of the dispersive dependence of a material as possible. However, fitting the actual data by (7) may result in the appearance of physically meaningless resonance frequencies.

The determination of Acher's constant from the Lorentzian curve fitting of the measured frequency dependence was used in a number of publications.^{14,24,29} In the present paper, we apply numerical modeling to justify the possibilities and determine the limits of applicability of Acher's constant extraction from experimental data obtained over a limited frequency range and having comparatively wide magnetic loss peak.

In Section II, it is shown that if the Gilbert parameter α is small, high-frequency permeability of the material is close to the limiting value, and if there is equality sign in (2), then the permeability is accurately described by the Lorentzian dispersion law. Further, the paper discusses possible physical reasons of noticeable distortions of the actual frequency dependence as compared to the Lorentzian dispersion law. Section II considers the case of high damping in the LLG frequency dependence. Section III describes the case when the effect of eddy currents is essential. In Section IV, the material inhomogeneity effect upon the dispersion law is discussed; the inhomogeneous material herein is modeled using the asymmetric Bruggeman mixing rule. For each of these cases, the feasibility of fitting the magnetic frequency dispersion by the Lorentzian dispersion law is analyzed. Also, the determination of Acher's constant of a magnetic material from the data available over a limited frequency range is discussed. Acher's constant may be found either by direct integration with the use of integral (4), or by curve fitting the real frequency dependence by the Lorentzian law following by calculating the constant for the fitting curve. It is shown that the divergence of the integral (3) is not observed within a realistic range of parameters and that the main difficulty is slow convergence of integral (4) to Acher's constant of the material. In all the cases, the application of curve fitting of frequency dependences results in more accurate determination of Acher's constant.

Preliminary results of the study have been published in Refs. 38 and 39.

II. THE LANDAU-LIFSHITZ-GILBERT LAW OF FREQUENCY DISPERSION

Fitting the calculated frequency dependences of permeability by the Lorentzian dispersion law is done using standard curve fitting techniques (in particular, non-linear least-

squares approach in regression analysis, though other curve fitting and optimization techniques could be used⁴⁰), under assumption that $\mu_\infty = 1$. For curve fitting, the permeability data arrays were calculated with a logarithmic frequency scale. The results are represented below as functions of the upper boundary of the frequency range, f_{\max} , in which the permeability data are available. The lower frequency limit is 0.1 GHz in all calculations below.

A. The shape of frequency dispersion of permeability

The LLG (6) and the Lorentzian (5) dispersion laws differ by the presence of an additional frequency-dependent term in the numerator. If this term is omitted, then the frequency characteristics in (5) and (6) coincide provided that

$$\begin{aligned} \mu_s - 1 &= 4\pi\gamma M_0/f_x, & f_{\text{res}}^2 &= f_x f_y / (1 + \alpha^2), \\ 1/f_{\text{rel}} &= \alpha (1/f_x + 1/f_y). \end{aligned} \quad (8)$$

Based on the second equation in (8), the conclusion is made in Refs. 15 and 21 that damping reduces K_A by the factor of $(1 + \alpha^2)$.

The Lorentzian and LLG dispersions coincide at $\alpha = 0$, and it is usually assumed that these two dispersion laws agree well at $\alpha \ll 1$. However, this is not exactly factual. The shapes of the magnetic loss peaks obtained from (5) and (6) are the same when the second term in the numerator of (6) is small as compared to the first term in the vicinity of f_{res} . Evaluating the value f_{res} as in (8), it is readily concluded that the shapes of the magnetic loss peaks are close if

$$\sqrt{f_y/f_x} \gg \alpha / (1 + \alpha^2). \quad (9)$$

Therefore, the Lorentzian dispersion law approximates the solution of the LLG equation accurately enough for any arbitrary value of the Gilbert parameter α when $f_y/f_x \gg 1$. This agrees with the condition of attaining high dynamic permeability, when the equality in (2) holds. The conclusion is that the Lorentzian dispersion law (5) is capable of close fitting the frequency-dependent permeability in the cases when the material has high dynamic permeability satisfying Acher's law, even if $\alpha \sim 1$.

This is illustrated by Fig. 1 that shows the comparison of the frequency dispersions (6) and (5) for $f_y/f_x \gg 1$ and $f_y/f_x = 1$. In both the cases, $\alpha = 1$ and the parameters are chosen in such a way that the peak of magnetic loss is close to 1 GHz. The Lorentzian frequency dependences shown in Fig. 1 as the dashed lines are obtained using numerical curve fitting of calculated LLG dependence by (5) with $\mu_\infty = 1$ and $f_{\max} = 3$ GHz. If $f_y = 10 \times f_x$, then both curves are close to each other, and the parameters of the curve-fitting Lorentzian dependence agree well with (8). When $f_y = f_x$, the shapes of the curves are markedly different, and Eq. (8) yields the Lorentzian parameters deviating greatly from those obtained by fitting.

B. Determination of Acher's constant

Accurate determination of Acher's constant using Eq. (4) requires the frequency f_{\max} to be high enough for the

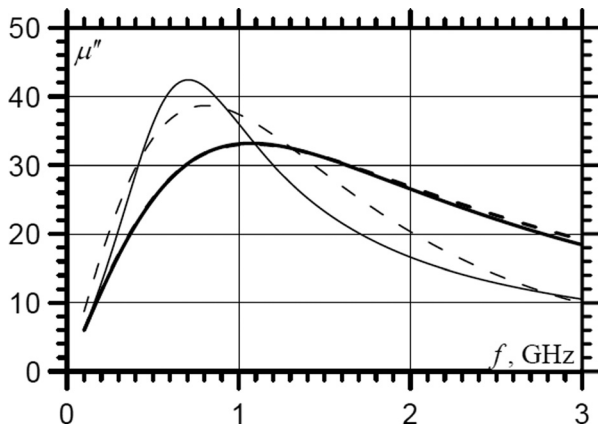


FIG. 1. Solid lines: frequency dependence of imaginary part of permeability corresponding to the LLG dispersion (6) with $4\pi\gamma M_0 = 60$ GHz, $f_x = 1$ GHz, $\alpha = 1$, and $f_y = 1$ GHz (thin line) and $f_y = 10$ GHz (thick line). Dashed lines: the result of the numerical curve fitting of the solid lines by Lorentzian dispersion law (5).

integral in the right-hand side of (4) to be independent of f_{\max} . In the case of the Lorentzian frequency dependence, this condition is determined by dissipation in the material only. A simple estimation of the effect of dissipation on the convergence of Acher’s integral is obtained by integrating the high-frequency asymptote of loss in Eq. (5): for $f \rightarrow \infty$, the asymptotic of normalized Acher’s integral is given by

$$i_A(f_{\max}) = 1 - \frac{2}{\pi} \frac{f_{\text{res}}^2}{f_{\max} f_{\text{rel}}}. \quad (10)$$

As is seen from (10), calculation of Acher’s constant K_A at high attenuation by direct integration of magnetic loss over a limited frequency range may result in a large uncertainty. The value of i_A is close to the unity when $f_{\max}/f_{\text{res}} \gg (2/\pi) (f_{\text{res}}/f_{\text{rel}})$. If α is high, then the loss peak is close to f_{rel} , while the frequency f_{res} is substantially higher, and the maximum frequency of integration f_{\max} should be even higher than f_{res} .

In contrast to the Lorentzian dispersion, LLG dispersion law (6) leads to the divergence of integral (3). Hence, the integral must exceed the limit established by Acher’s law. Application of Eq. (4) for the analysis of permeability in this case is feasible if the frequency range is found, where Acher’s integral reaches saturation, i.e., varying slightly with frequency. For saturation, two conditions must be fulfilled. First, the integral of the second term in (6) should be lower than the limiting value determined by the first term; this means that the frequency should not be too high. Second, the frequency should not be too low either to assure for reaching the limiting value.

The first of these conditions,

$$f \ll f_y/\alpha, \quad (11)$$

follows from the asymptotic expression for the imaginary permeability at $f \rightarrow \infty$ and the limiting value of Acher’s constant obtained by substituting (8) to (2).

The second condition is written based on (10) and (8) as

$$f \gg \frac{\alpha}{1 + \alpha^2} (f_x + f_y). \quad (12)$$

As follows from (11) and (12), the frequency range, where integral (4) is almost independent of frequency, emerges, when:

$$\frac{\alpha^2}{1 + \alpha^2} \ll \frac{f_y}{f_x + f_y}. \quad (13)$$

Inequality (13) is held only for $\alpha \ll 1$ independently of the f_y/f_x value. Therefore, Acher’s integral can be used for the analysis of experimental data only for low α .

Figure 2 shows the results of Acher’s constant computations over a limited frequency range for the LLG frequency dependence. The left-hand side of the figure shows the data for the case of $f_y/f_x \gg 1$, when LLG and Lorentzian frequency dependences do not differ much. It is seen from the plot that calculation of Acher’s constant by integration (shown by the solid line) results in just rough estimation at $\alpha = 0.1$. At higher loss constants, e.g., $\alpha = 0.5$, dependence $i_A(f)$ does not allow for making any conclusion about the value of K_A . However, fitting the actual frequency characteristic by the Lorentzian dispersion law, as is plotted by the dashed line, provides an accurate value of Acher’s constant;

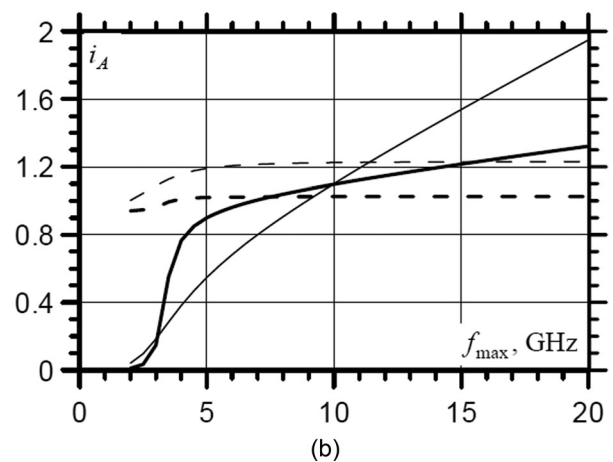
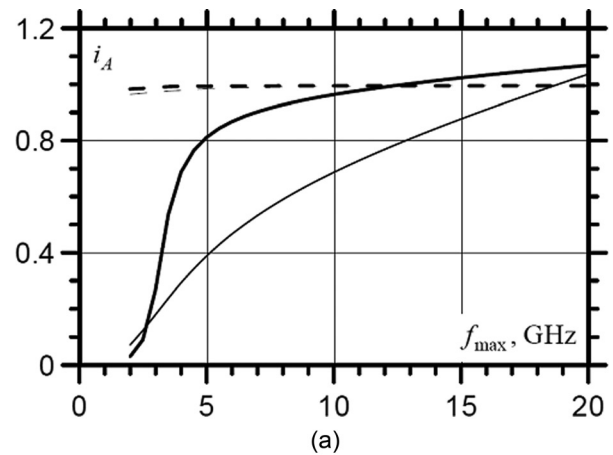


FIG. 2. Normalized Acher’s integral (4) calculated for the LLG dispersion law (solid lines) with (a) $4\pi\gamma M_0 = 60$ GHz, $f_x = 10$ GHz, and $f_y = 1$ GHz, and (b) $4\pi\gamma M_0 = 60$ GHz, $f_x = 3.3$ GHz, and $f_y = 3.3$ GHz. The damping parameter is $\alpha = 0.1$ (thick lines) and $\alpha = 0.5$ (thin lines). The dotted lines are the result of fitting by Lorentzian dispersion law (5) over a limited frequency range.

this is true even with $f_{\max} = 2$ GHz, when the resonance frequency is higher than f_{res} .

The right-hand plot corresponds to the case when $f_y = f_x$. Herein, the uncertainty of determination of Acher's constant by integration is much higher; as a matter of fact, Acher's constant cannot be determined by this way. For the low-loss case, fitting by the single-term Lorentzian dispersion law is still reasonable. At the higher loss, $\alpha = 0.5$, the fitting inaccuracy is large, and the result is $i_A = 1.23$, which exceeds the ultimate value following from Eq. (4), the unity. The use of multiple terms in the Lorentzian fitting of LLG frequency dependence may cause even higher inaccuracy. The reason is that the additional resonances in the multi-term Lorentzian dependence contribute to the enhanced high-frequency loss in LLG, which results in the higher value of the Acher's constant as compared to the single-term Lorentzian dispersion.

Note that in the case considered above, Acher's constant is determined accurately by Eq. (2) provided that f_{res} is defined as the frequency where $\mu' = 1$ rather than the frequency of maximum magnetic loss as is usually assumed. Such definition yields the data coinciding with the results of Lorentzian fitting with $n = 1$, including the case of high damping shown in the right-hand plot in Fig. 2, where fitting produces an overestimated value of i_A . This overestimation can be explained as follows. Since the real permeability in the LLG dispersion equals to one at the frequency

$$f|_{\mu'=1} = 1 + f_y \sqrt{f_x} / \sqrt{f_y - f_x \alpha^2}, \quad (14)$$

then, for $f_y/f_x < \alpha^2$, the real permeability given by the LLG dispersion law is greater than the unity at any frequency.

The results obtained indicate that Acher's constant is independent of the Gilbert parameter α , in contrast to the conclusions given in Refs. 15 and 21. However, the very fact that the value of α in LLG dependence is small ($\alpha < 0.1$) makes this problem not that important. Also, for this reason, Lorentzian dispersion law (5) is used below to model the permeability frequency dependences. For the sake of simplicity, we employ the single-term Lorentzian law to model the FMR in a magnetic material.

Note also that the Landau-Lifshitz equation with the Gilbert damping term may be considered as a frequency dependence of magnetic anisotropy field represented as a series at low frequencies. Current literature discusses a possibility of accounting for higher-order terms in the series,³⁷ or, equivalently, introducing the frequency dependence of the damping parameter.^{20,41} This may be associated with the fact that the LLG dispersion law is valid only at frequencies below and in the vicinity of the FMR, and therefore the divergence of integral (3) for LLG dispersion requires further investigation.

III. THE CASE OF STRONG SKIN EFFECT

The skin effect results in a distortion of frequency dependence of permeability. The standard approach of taking the skin effect into account is a re-normalization of the intrinsic permeability of a conducting particle μ_i into the apparent permeability μ , which is a measurable value, see,

e.g., Ref. 42. For the sake of definiteness, let us consider the renormalization for a thin magnetic film, when μ and μ_i are related as

$$\mu = \mu_i \frac{\tan\left((1+i)\pi a \sqrt{\mu_i \sigma f} / c\right)}{(1+i)\pi a \sqrt{\mu_i \sigma f} / c}, \quad (15)$$

where a and σ are its thickness and ohmic conductivity, respectively. Even for the materials without any intrinsic magnetic loss, where μ_i equals to the static permeability μ_s , a loss peak of apparent permeability appears due to the skin effect at frequency f_δ , which corresponds to the skin depth equal to $a/2$

$$f_\delta = (c/a)^2 / (8\mu_s \sigma). \quad (16)$$

Frequency f_δ will be further referred to as the "skin frequency." The correlation between f_δ and f_{res} determines how strongly the skin effect contributes to the shape and location of magnetic loss peak. The loss peak is determined mainly by the FMR at $f_\delta \gg f_{\text{res}}$ and by the skin effect at $f_\delta \ll f_{\text{res}}$.

Below, the single-term Lorentzian dispersion law (5) is used in all the examples to describe frequency dependence of the intrinsic permeability.

A. The shape of frequency dispersion of permeability

The Lorentzian frequency dependence is defined by a pole determined by characteristic frequencies f_{res} and f_{rel} . Similarly, the frequency dependence of the apparent permeability is determined by the poles of the right-hand side of (15), i.e., the complex frequencies, where the argument of the tangent is an odd multiple of $\pi/2$. If the optical permeability μ_∞ is negligible as compared to the static permeability, then, according to (15), the skin effect transforms the Lorentzian pole of the intrinsic permeability to an infinite series of the poles of the apparent permeability determined by characteristic frequencies $f_{\text{res},j}$ and $f_{\text{rel},j}$

$$\frac{1}{f_{\text{rel},j}^*} = \frac{1}{f_{\text{rel}}} + 8 \frac{\mu_s a^2 \sigma}{(2j-1)^2 c^2} = \frac{1}{f_{\text{rel}}} + \frac{1}{(2j-1)^2 f_\delta}, \quad f_{\text{res},j}^* = f_{\text{res}}, \quad (17)$$

where f_δ is determined by (16), $j = 1, 2, \dots, \infty$, and $\mu_s \gg 1$ is assumed. The partial susceptibilities corresponding to the poles are calculated through the residues in the poles, which results in proportionality of their amplitudes to $(2j-1)^2$.

Therefore, fitting a frequency dependence of apparent permeability by generalized Lorentzian dispersion law (7) may be accurate enough when keeping just a few first Lorentzian terms. This is illustrated by Fig. 3 that shows that the frequency dependence of permeability obtained with the account for the skin effect is closely fitted by a sum of just two Lorentzian terms. It is seen from the figure that the skin effect results in splitting of the FMR into two distinct peaks, see solid curves. The low-frequency peak is located at frequency f_δ , and the high-frequency peak is associated with the intrinsic resonance (natural FMR) of the bulk material. The dashed lines in Fig. 3 show the result of fitting the solid lines

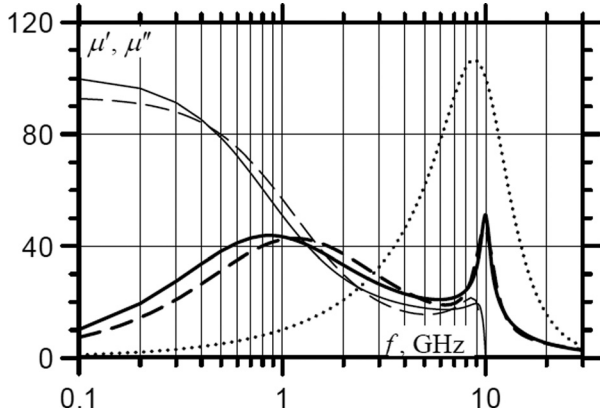


FIG. 3. Solid lines: real (thin line) and imaginary (thick line) parts of apparent permeability calculated using (15) with $f_\delta = 1$ GHz under assumption that the intrinsic permeability is described by the Lorentzian dispersion with $\mu_s = 100$, $f_{\text{res}} = f_{\text{rel}} = 10$ GHz, and $\mu_\infty = 1$. Dotted line: the imaginary part of intrinsic permeability. Dashed lines: the result of fitting the apparent permeability by the sum of two Lorentzian terms ($n = 2$) in (7).

by a sum of two Lorentzian terms, $n = 2$ in (7). The resonance frequency of both fitting resonances is close to the FMR frequency of the permeability of the bulk material. The relaxation frequency of the low-frequency resonance is close to f_δ and corresponds to the case of $j = 1$ in (17). The high-frequency peak is the result of averaging the higher-order terms ($j > 1$) given by (17).

B. Determination of Acher's constant

The previous discussion shows that the skin effect does not change the resonance frequency determined by the condition $\mu' = 1$. Since the skin effect does not change μ_s either, the conclusion has been made that application of Acher's law (2) and (3) is not affected by the skin effect.⁴⁰ However, this is not quite true. Equation (17) is obtained by neglecting the optical permeability, μ_∞ . Accounting for it leads to cumbersome mathematical expressions. For the sake of simplicity, it is reasonable to consider another limiting case instead, when the frequency-dependent second term in (5) is small as compared to the frequency-independent optical permeability. In this case, it is readily obtained that the poles of the apparent permeability have the infinite resonance frequency, which leads to the divergence of the integral in the right-hand side of (3). As the frequency increases, the frequency-dependent term in (6) is low as compared to the frequency-independent term, and the integral in the right-hand side of (3) diverges. Therefore, integral (3) always diverges in the presence of skin effect. Notice that the magnetic loss peak appears even in non-magnetic conductors, and it is the skin effect that is responsible for the appearance of non-unity dynamic permeability in metals.⁴³

To evaluate the contribution of these poles to (3), let us consider the first pole ($j = 1$) and assume that its magnitude corresponds to the static permeability equal to the unity. Then the relaxation frequency for this pole is f_δ , and the contribution of the pole to integral (4), which equals to $(2/\pi)f \times f_\delta$, is on the order of K_A at

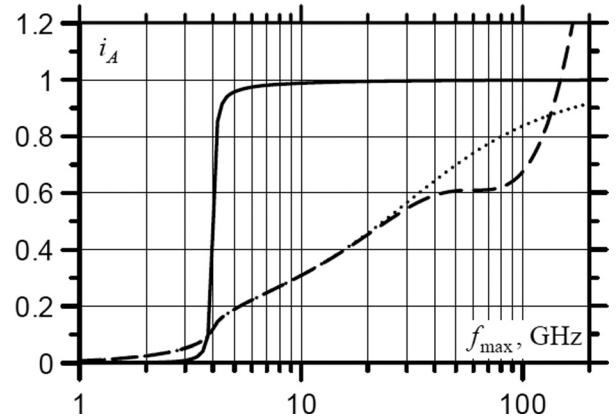


FIG. 4. Calculated dependences $i_A(f_{\text{max}})$ for Lorentzian dispersion law (5) with $\mu_s = 225$, $f_{\text{res}} = 4$ GHz, $f_{\text{rel}} = 100$ GHz, and $\mu_\infty = 1$ (solid line); for the apparent permeability calculated with the above parameters and with skin frequency $f_\delta = 0.5$ GHz (dashed line); for the apparent permeability calculated with the above parameters and with skin frequency $f_\delta = 0.5$ GHz under assumption that $\mu_\infty = 0$ (dotted line).

$$f \sim (\pi/2)f_{\text{res}}^2/f_\delta. \quad (18)$$

For materials with high static permeability, this frequency is substantially high.

Figure 4 illustrates the convergence of Acher's integral for the case of skin effect. The solid line shows the dependence $i_A(f)$ calculated for Lorentzian dispersion law (5) at $\mu_s = 225$, $f_{\text{res}} = 4$ GHz, $f_{\text{rel}} = 100$ GHz, and $\mu_\infty = 1$. The dashed line shows the dependence of the apparent permeability obtained from this Lorentzian curve by (15) with $f_\delta = 0.5$ GHz. It is seen that the curve goes up rapidly at frequencies above 100 GHz, which is due to the divergence of Acher's integral caused by the skin effect. Equation (18) yields 50 GHz for these parameters; taking into account the assumptions at the derivation of (18), the comparatively good agreement has been achieved between this value and the frequency, at which the divergence of Acher's integral becomes noticeable, as is shown in Fig. 4. The dotted line in the figure shows the calculated results obtained under assumption that $\mu_\infty = 0$. In this case, the assumption at which Eq. (17) has been derived is valid at any frequency, and normalized Acher's integral converges to the unity rather than increases rapidly at high frequencies. Therefore, the divergence of Acher's integral caused by the skin effect appears at substantially high frequencies. In the microwave region, Acher's integral may be useful in the analysis of the magnetic properties of materials.

Note that the dashed and the dotted curves differ also in the frequency range from 40 to 120 GHz. This difference appears at frequencies where the real part of intrinsic permeability is close to zero. In this frequency region, the skin depth drastically increases, and the loss associated with the skin effect consequently reduces. This causes the slower growth in the integral value shown as the dotted line that may be confused with the saturation of the integral. At $\mu_\infty = 0$, the real part of the intrinsic permeability is always below zero at the frequencies above the FMR, and such effect does not show up. This discrepancy cannot be predicted based on the simplified mathematical formulation of the skin effect used above.

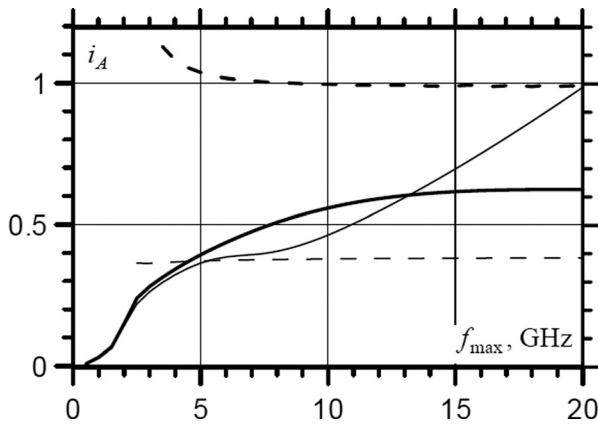


FIG. 5. Acher's constant in the case of skin effect. Solid lines: calculation by integration for $\mu_{s,i} = 100$, $f_{\text{res}} = 2$ GHz, $f_{\text{rel}} = 50$ GHz, $f_{\delta} = 0.4$ GHz (thick line), and for $\mu_{s,i} = 10$, $f_{\text{res}} = 2$ GHz, $f_{\text{rel}} = 10$ GHz, $f_{\delta} = 0.4$ GHz (thin line). Dashed lines: calculation based on the Lorentzian fitting for the same set of parameters.

It is also important to note the very slow convergence of Acher's integral for the case of skin effect, which is seen in Fig. 4. According to (17), the skin effect is equivalent to a reduction of the relaxation frequency in the representation of the apparent permeability by the Lorentzian dispersion. This, in turn, affects the convergence rate of Acher's integral according to (10). The high-frequency loss of apparent permeability is determined mainly by the magnetic loss peak associated with the skin effect and located at f_{δ} , as is seen from Fig. 3.

Figure 5 shows Acher's constant calculated over a limited frequency range with the account for the skin effect. In the calculations, the frequency dependence of intrinsic permeability is assumed to obey the Lorentzian law with $f_{\text{res}} = 2$ GHz. The intrinsic permeability and the electric conductivity are chosen such that $f_{\delta} = 0.4$ GHz, which means that the skin effect is essential. The calculated results are plotted against the higher frequency where the permeability is available, f_{max} . Solid lines show the result obtained by integration of the imaginary part of apparent permeability, according to (4). Dashed lines are calculated from the Lorentzian fits of the frequency dependence of apparent permeability. Since the skin effect results in the appearance of two magnetic loss peaks, Lorentzian fitting of the apparent permeability is made with $n = 2$ in (7).

Thick lines in Fig. 5 show the calculated results for the case of high static permeability and high quality factor (Q -factor) magnetic resonance, $\mu_s = 100$ and $f_{\text{rel}} = 50$ GHz. In this case, according to the above discussion, the integration results in significantly lowered values of K_A at all values of f_{max} up to 20 GHz. Fitting yields the values close to the unity at $f_{\text{max}} > 4$ GHz. At lower f_{max} , the procedure produces overestimated values of K_A . The reason is that if the resonant frequency is close to f_{max} , then its determination by fitting becomes less accurate. If $f_{\text{res}} > f_{\text{max}}$, fitting does not allow for determining the resonance frequency at all. In this case, the fitted resonance frequency typically tends to be very high because the frequency dependence of apparent permeability is distorted relatively to the Lorentzian line. Therefore, Acher's constant obtained by fitting may be much higher than the unity in this case.

If $f_{\text{res}} < f_{\text{max}}$, then fitting yields rather accurate result. The physical reason for this is as follows. As is seen from integrals (3) and (4), the values of μ'' at high frequencies give the dominant contribution to the value of Acher's integral. When the imaginary permeability is integrated over a limited frequency range, the permeability at higher frequencies is neglected, which produces an underestimated value of K_A . The calculation of Acher's constant by fitting implies some assumptions regarding the high-frequency asymptotes of the permeability. The skin effect results in the appearance of large high-frequency loss, which decays slowly with frequency. This behavior is consistent with the Lorentzian frequency dispersion law.

As the amplitude and Q -factor of the resonance of intrinsic permeability reduce, the accuracy of determination of Acher's constant also becomes lower. Thin lines in Fig. 5 show the calculated results with $\mu_s = 10$ and $f_{\text{rel}} = 10$ GHz. In this case, fitting yields the substantially low value of normalized Acher's constant, of about 0.4. This value is even lower than the one produced by the integration. On the other hand, the integration gives a value that depends on f_{max} : at $f_{\text{max}} = 20$ GHz, Acher's constant equals to the unity and continues to rise with frequency. Therefore, at these parameters of the problem, none of the approaches under consideration allow for determining Acher's constant.

Notice that in the case of the skin effect, application of (2) yields good results again. If the intrinsic permeability is high, then the frequency, where the real permeability is equal to zero, is identical for both intrinsic and apparent permeabilities. The static values of these are equal as well. Because of this, even in the case of low amplitude and low Q -factor considered above, Eq. (2) produces $K_A = 1.03 \times (\gamma 4\pi M_0)^2$.

IV. THE CASE OF INHOMOGENEOUS MATERIALS

Mixing rules developed in the theory of composites are employed herein to study an opportunity of obtaining accurate values of Acher's constant in inhomogeneous materials. The comprehensive review of the state-of-art in the field of mixing rules is found, e.g., in Refs. 44 and 45. It is well known that the application of any mixing rule, except for the Maxwell Garnett theory, to the Lorentzian frequency dependence results in the appearance of a continuous set of resonance frequencies associated with the effective permeability. We use Bruggeman's Effective Medium Theory (EMT)⁴⁶ as a model for an inhomogeneous magnetic material. In the EMT, the effective permeability μ_{eff} of a composite consisting of a non-magnetic matrix and magnetic inclusions is found from the following equation:

$$p \frac{\mu_i - \mu_{\text{eff}}}{\mu_{\text{eff}} + N(\mu_i - \mu_{\text{eff}})} + (1 - p) \frac{1 - \mu_{\text{eff}}}{\mu_{\text{eff}} + N(1 - \mu_{\text{eff}})} = 0. \quad (19)$$

In Eq. (19), N is the demagnetization factor of magnetic inclusions along the incident magnetic field, p is the volume factor of inclusions, and μ_i is the intrinsic permeability of inclusions. If the skin effect in the inclusions is essential, the

apparent permeability renormalized according to Eq. (15), μ , must be used.

The EMT results in a broad distribution of effective resonance frequencies of effective permeability at concentrations close to the percolation threshold, $p_c = N$. Using the Bergman–Milton spectral theory,⁴⁷ it is readily shown that if $p \sim p_c$, then the effective resonance frequencies are located in the range from f_{res} to

$$\hat{f}_{\text{res}} = f_{\text{res}} \sqrt{1 + \mu_s}, \quad (20)$$

where f_{res} is the resonance frequency and μ_s is the static value of the intrinsic permeability of the bulk material of inclusions.

It is known^{20,29} that the value of K_A for the effective permeability calculated using any mixing rule equals to Acher's constant of inclusions multiplied by the volume concentration p . Therefore, the integral always converges provided that it converges for the intrinsic permeability. It is also known that the EMT is consistent only if $N = 1/3$; i.e., the inclusions are of spherical shape. It is the value that is assumed in the calculations below, though, strictly speaking, the demagnetization factor in a mixing rule should be consistent with that involved in the LLG equation for the intrinsic permeability of inclusions.¹¹ To satisfy Acher's law, this demagnetization factor must be low. Moreover, the effective properties of composites containing inclusions with low demagnetization factors typically obey the Wiener mixing rule.⁴⁸ However, the Wiener mixing rule does not introduce any distortion of the frequency dependence of effective permeability as compared to the frequency dependence of intrinsic permeability and therefore is not useful for the analysis given in this section. Therefore, the EMT is employed below to illustrate the effect of the distribution of the resonance frequencies on the determination of K_A , and the considered frequency dependences of effective permeability may not be consistent with the performance of real composite materials.

A. The shape of frequency dispersion of permeability

Figure 6 shows the frequency dependence of the effective permeability calculated using the EMT (19) with $p = 0.25$ and $N = 1/3$ under assumption that the intrinsic permeability of inclusions is governed by Lorentzian dispersion law (5) with $\mu_s = 100$, $f_{\text{res}} = 1$ GHz, $f_{\text{rel}} = 10$ GHz, see solid lines. The dashed and dotted lines show the results of fitting of the calculated curve by Lorentzian dependence (7) for $n = 1$ and $n = 2$, respectively. It is seen that the EMT does yield the strong distortion of the Lorentzian dependence at the concentrations close to the percolation threshold, and the Lorentzian fitting does not allow for obtaining perfect agreement between the calculated effective permeability and its Lorentzian fitting even with $n = 2$. It is readily shown from the Bergman–Milton approach that the EMT implies that the resonance frequencies are distributed over a wide frequency range but have high Q -factors. Fitting these multiple resonances with two Lorentzian terms requires the quality factor of these resonances to be low, as the magnetic loss

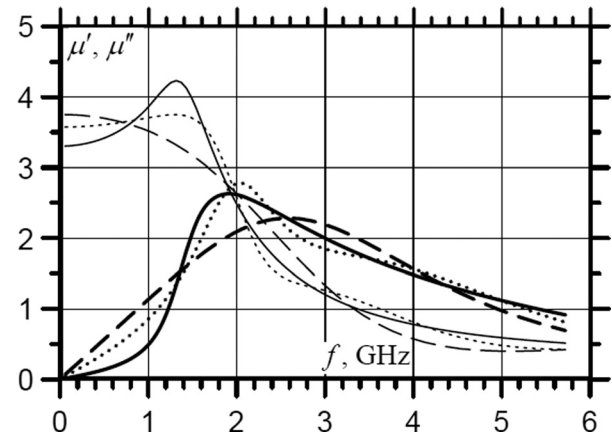


FIG. 6. Solid lines: the frequency dependence of effective permeability of a composite material calculated using EMT (19) with $p = 0.25$ and $N = 1/3$ from Lorentzian dispersion law (7), with $\mu_s = 200$, $f_{\text{res}} = 1$ GHz, and $f_{\text{rel}} = 10$ GHz. Dashed lines: the one-term ($n = 1$) Lorentzian fitting of the calculated dependence. Dotted lines: the two-term ($n = 2$) Lorentzian fitting of the calculated dependence. Thick lines correspond to the imaginary permeability, and thin lines to the real permeability.

covers a wide frequency range. For this reason, the exact shapes of the fitted and fitting curves differ, and the accuracy of fitting is low. The fitting accuracy will definitely be enhanced with the larger number of the Lorentzian terms. However, from the standpoint of determining of Acher's constant, fitting with a large number of Lorentzian terms may result in the increased uncertainty, because this may reduce the accuracy of determining the resonant frequencies. As a result, some of the resonant frequencies may go above f_{max} , which results in a drastic increase of the calculated Acher's constant, as is explained in Section III.

B. Determination of Acher's constant

Figure 7 shows the calculation results for Acher's constant of inhomogeneous material plotted against the upper boundary of the operational frequency range f_{max} , where the data on the permeability are available. The solid lines represent the results obtained by the integration using Eq. (4) for two cases. The thin line shows the effective permeability calculated by the EMT at $N = 1/3$ and $p = 0.25$ from the Lorentzian frequency dependence of the intrinsic permeability with $\mu_s = 200$, $f_{\text{res}} = 1$ GHz, and $f_{\text{rel}} = 10$ GHz. The second case shown by thick line employs the same set of parameters, but accounts for the skin effect with $f_{\delta} = 0.11$ GHz. The corresponding dashed lines show the results obtained for these cases by Lorentzian fitting with $n = 2$.

When the skin effect is neglected, computations of i_A by integration yield the value close to the unity at $f_{\text{max}} \sim 13$ GHz, which agrees with \hat{f}_{res} . At lower f_{max} , fitting produces more accurate results than the integration, with the deviation from the unity being approximately twice as low. The result is similar when the skin effect is accounted for, with the only difference that the integration gives underestimated values of i_A , of about 0.7, at high values of f_{max} . Therefore, the Lorentzian fitting allows the accuracy of Acher's constant extraction to be increased in the case of inhomogeneous materials as well.

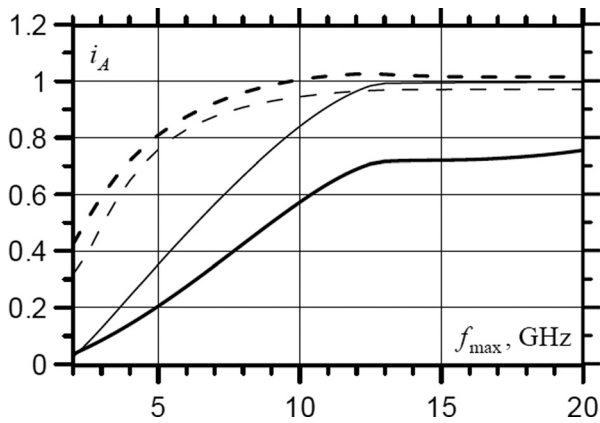


FIG. 7. Calculation of Acher's constant for an inhomogeneous material. Solid lines: the result of integration with $N=1/3$, $p=0.25$, $\mu_s=200$, $f_{\text{res}}=1$ GHz, and $f_{\text{el}}=10$ GHz (thin line); for the same set of parameters with the account for the skin effect with $f_\delta=0.11$ GHz (thick line). Dotted lines: calculation by the Lorentzian fitting with $n=2$; thin and thick lines correspond the same parameters as above.

The only occasion when the integration produces slightly more accurate Acher's constant than fitting is the case of $f_{\text{max}} > f_{\text{res}}$. This can be explained as follows. The application of the Lorentzian fitting is based on the predicted behavior of permeability beyond the boundaries of the frequency range. Strictly speaking, this dependence is unknown, and any scenario is possible—from a drastic reduction of loss (down to zero) at frequencies above f_{max} , to an increase of loss resulting in enhanced values of K_A . Application of the Lorentzian fitting implicitly means that no resonances of permeability are expected at frequencies above f_{max} , so that the high-frequency asymptote of the permeability is associated only with “tails” of the resonances located in the operational frequency range. If this band is substantially wide, and fitting involves two Lorentzian terms, these terms should have comparatively low Q -factor to assure for sufficient loss over the entire frequency range. If the skin effect is a dominant factor in magnetic loss, the assumption of a low Q -factor is plausible, because the high-frequency loss is mainly due to the low-frequency loss peak that has a low quality factor. When the magnetic peak is spread because of inhomogeneities, a continuous spectrum appears. The latter consists of absorption lines, the quality factors of which increase with the resonance frequency, starting from the comparatively high Q -factor of the initial magnetic spectrum. Therefore, the magnetic loss drastically reduces at frequencies above the highest resonance of the effective permeability. This reduction cannot be described by the low-frequency fitting resonances, and therefore the overestimated values of K_A may appear.

The application of (2) for an inhomogeneous material leads to the incorrect evaluation of Acher's constant. For example, for the data from Fig. 7, the application of (2) results in $i_A=0.32$ for case when the skin effect is neglected, and $i_A=0.44$ for the case when the skin effect is accounted for. The reason is that the averaged resonance frequency may greatly differ from the frequency, where the real magnetic susceptibility crosses zero, in the case of wide distribution of the resonances. This issue was first addressed in Ref. 6 when analyzing Snoek's law in inhomogeneous materials.

V. CONCLUSION

The promising usefulness of application of Acher's law for the analysis of measured permeability data is widely discussed in literature. However, two factors limit its applicability. The first of these is that Acher's law is rigorously derived only for the case of a uniformly magnetized ellipsoidal particle, without accounting for its domain structure, skin effect, presence of pores and defects, etc. Equation (2) is applicable to only high-quality FMR without any splitting or distortion of the resonance peak. Second, Acher's integral that is used for calculations of Acher's constant for the case of complicated frequency dispersions converges slowly in many cases. Since any measured data are available only for a limited frequency range, this reduces the accuracy of evaluation of Acher's constant.

This paper discusses an opportunity of accurate estimating Acher's constant in the cases when the frequency dependence of permeability has large width or distorted shape. It is shown that for the LLG dispersion law, which describes the FMR, the integral Acher's law is inapplicable, since the integral diverges. However, as a rule, for data obtained in a realistic frequency range, the main challenge is the slow convergence of the integral rather than the divergence. It is also shown that if the practically important case of high microwave permeability is under consideration, then the LLG dispersion law is close to the Lorentzian dispersion law, which makes Acher's integral applicable.

Possible reasons of distortion of frequency characteristics of permeability may be the skin effect in a conducting ferromagnetic material, as well as inhomogeneity of the material. The skin effect causes the divergence of Acher's integral; the integral grows steadily with frequency and no saturation to an asymptotic value is observed. This prevents from estimating the actual value of Acher's constant from measured data over a limited frequency range.

For all these cases, we have tested a possibility of extracting Acher's constant from measured/available frequency-dependent permeability data over a limited frequency range. The standard method of obtaining Acher's constant by the integration of magnetic loss over the frequency range is considered, as well as an alternative technique which employs the Lorentzian fitting of the measured frequency dependence and search of Acher's constant based on the parameters of fitting curve. The latter technique has not been experimentally validated or theoretically justified in the literature yet. In the majority of the studied cases, the curve fitting by the Lorentzian dispersion law produces Acher's constant which is closer to the true value as compared to the integration. The reason is that fitting accounts, at least partially, for magnetic loss located beyond the operational frequency range. As a matter of fact, the curve fitting uses the data on the real part of permeability for evaluating the high-frequency asymptote of the imaginary permeability, which allows for obtaining the improved accuracy. The accuracy improvement may also be attained by more sophisticated approaches, such as those based on Kramers-Kronig relations.⁴⁹ However, various curve fitting algorithms, e.g., employing the genetic algorithms, or linear and non-linear regression analysis,³⁸ are much simpler in realization.

Note that the application of the curve fitting over a narrow operational frequency range may result in a much higher resonance frequency of the fitting curve and, therefore, in a substantially overestimated value of Acher's constant. Obviously, the same uncertainty may be caused by large inaccuracy in the frequency dependence of permeability. In contrast, the integration usually yields underestimated results.

In a number of cases, an accurate determination of Acher's constant is feasible by using Eq. (2) based on the values of static permeability and resonance frequency, which is defined as the frequency where the real part of permeability crosses the unity. However, as is shown above, this approach fails for inhomogeneous materials. In addition, it employs just two characteristic points in the frequency dependence of permeability rather than the entire dependence and therefore should be much more sensitive to measurement errors.

ACKNOWLEDGMENTS

The study was performed with partial financial support from the Russian Foundation for Basic Research, Project No. 15-08-03535, and it was supported in part by the National Science Foundation (USA) under Grant No. IIP-1440110.

- ¹I. T. Iakubov, A. N. Lagarkov, A. V. Osipov, S. A. Maklakov, K. N. Rozanov, I. A. Ryzhikov, and S. N. Starostenko, *AIP Adv.* **4**, 107143 (2014).
- ²J. L. Snoek, *Physica* **14**, 207 (1948).
- ³G. Perrin, O. Acher, J. C. Peuzin, and N. Vucadinovich, *J. Magn. Magn. Mater.* **157/158**, 289 (1996).
- ⁴R. M. Walser, W. Win, and P. M. Valanju, *IEEE Trans. Magn.* **34**, 1390 (1998).
- ⁵A. L. Adenot, O. Acher, T. Taffary, and L. Longuet, *J. Appl. Phys.* **91**, 7601 (2002).
- ⁶K. N. Rozanov, Z. W. Li, L. F. Chen, and M. Y. Koledintseva, *J. Appl. Phys.* **97**, 013905 (2005).
- ⁷J. Torrejon, A.-L. Adenot-Engelvin, F. Bertin, V. Dubuget, O. Acher, and M. Vazquez, *J. Magn. Magn. Mater.* **321**, 1227 (2009).
- ⁸K. N. Rozanov and S. N. Starostenko, *J. Commun. Technol. Electron.* **48**, 652 (2003).
- ⁹P. M. T. Ikonen, K. N. Rozanov, A. V. Osipov, P. Alitalo, and S. A. Tretyakov, *IEEE Trans. Antennas Propag.* **54**, 3391 (2006).
- ¹⁰A. Thiaville, N. Vukadinovic, and O. Acher, *Phys. Rev. B* **86**, 214404 (2012).
- ¹¹R. Ramprasad, P. Zurcher, M. Petras, M. Müller, and P. Renaud, *J. Appl. Phys.* **96**, 519 (2004).
- ¹²G. Z. Chai, D. S. Xue, X. L. Fan, X. L. Li, and D. W. Guo, *Appl. Phys. Lett.* **93**, 152516 (2008).
- ¹³O. Acher, V. Dubuget, and S. Dubourg, *IEEE Trans. Magn.* **44**, 2842 (2008).
- ¹⁴I. T. Iakubov, A. N. Lagarkov, S. A. Maklakov, A. V. Osipov, K. N. Rozanov, I. A. Ryzhikov, V. V. Samsonova, and A. O. Sboychakov, *J. Magn. Magn. Mater.* **321**, 726 (2009).
- ¹⁵N. A. Buznikov and K. N. Rozanov, *J. Magn. Magn. Mater.* **285**, 314 (2005).
- ¹⁶S. Ge, D. Yao, M. Yamaguchi, X. Yang, H. Zuo, T. Ishii, D. Zhou, and F. Li, *J. Phys. D: Appl. Phys.* **40**, 3660 (2007).
- ¹⁷K. Seemann, H. Leiste, and C. Klever, *J. Magn. Magn. Mater.* **322**, 2979 (2010).
- ¹⁸B. Viala, G. Visentin, and P. Gaud, *IEEE Trans. Magn.* **40**, 1996 (2004).
- ¹⁹Y. P. Wu, Y. Yang, Z. H. Yang, N. N. Phouc, F. S. Ma, B. Y. Zong, and J. Ding, *J. Appl. Phys.* **118**, 013902 (2015).
- ²⁰O. Acher and A. L. Adenot, *Phys. Rev. B* **62**, 11324 (2000).
- ²¹P. H. Zhou, T. Liu, J. L. Xie, and L. J. Deng, *J. Appl. Phys.* **111**, 113912 (2012).
- ²²P. H. Zhou and L. J. Deng, *IEEE Trans. Magn.* **45**, 663 (2009).
- ²³A. Bonneau-Braut, S. Dubourg, V. Dubuget, D. Plessis, and F. Duverger, *J. Phys.: Conf. Ser.* **303**, 012088 (2011).
- ²⁴M. Han, D. Liang, K. N. Rozanov, and L. Deng, *IEEE Trans. Magn.* **49**, 982 (2013).
- ²⁵C. P. Neo, Y. Yang, and J. Ding, *J. Appl. Phys.* **107**, 083906 (2010).
- ²⁶J. L. Wallace, *IEEE Trans. Magn.* **29**, 4209 (1993).
- ²⁷T. Taffary, D. Autisser, F. Boust, and H. Pascard, *IEEE Trans. Magn.* **34**, 1384 (1998).
- ²⁸I. T. Iakubov, A. N. Lagarkov, S. A. Maklakov, A. V. Osipov, K. N. Rozanov, I. A. Ryzhikov, N. A. Simonov, and S. N. Starostenko, *J. Magn. Magn. Mater.* **258–259**, 195 (2003).
- ²⁹A. N. Lagarkov, A. V. Osipov, K. N. Rozanov, and S. N. Starostenko, in *Proceedings of the 3rd International Conference on Materials for Advanced Technologies (ICMAT 2005) Symposium R: Electromagnetic Materials*, Singapore, 3–8 July 2005, pp. 74–77.
- ³⁰T. Nakamura, T. Tsutaoka, and K. Hatakeyama, "Frequency dispersion of permeability in ferrite composite materials," *J. Magn. Magn. Mater.* **138**, 319 (1994).
- ³¹M. Koledintseva, J. Drewniak, Y. J. Zhang, J. Lenn, and M. Thoms, *J. Magn. Magn. Mater.* **321**, 730 (2009).
- ³²I. T. Iakubov, A. N. Lagarkov, S. A. Maklakov, A. V. Osipov, D. A. Petrov, K. N. Rozanov, and I. A. Ryzhikov, *J. Magn. Magn. Mater.* **316**, e813 (2007).
- ³³T. Tsutaoka, *J. Appl. Phys.* **93**, 2789 (2003).
- ³⁴J. Huijbregtse, F. Roozeboom, J. Sietsma, J. Donkers, T. Kuiper, and E. van de Riet, *J. Appl. Phys.* **83**, 1569 (1998).
- ³⁵T. L. Gilbert, *IEEE Trans. Magn.* **40**, 3443 (2004).
- ³⁶M. Y. Koledintseva, J. L. Drewniak, D. J. Pommerenke, G. Antonini, A. Orlandi, and K. N. Rozanov, *IEEE Trans. Electromagn. Compat.* **47**, 392 (2005).
- ³⁷D. Botcher and J. Henk, *Phys. Rev. B* **86**, 020404 (2012).
- ³⁸M. Y. Koledintseva, J. Xu, S. De, J. L. Drewniak, Y. He, and R. Johnson, *IEEE Trans. Magn.* **47**, 317 (2011).
- ³⁹K. N. Rozanov and M. Y. Koledintseva, in *Proceedings of the IEEE International Symposium on Electromagnetic Compatibility*, Pittsburgh, USA, 5–10 August 2012, pp. 422–427.
- ⁴⁰K. N. Rozanov and M. Y. Koledintseva, in *Proceedings of the IEEE International Symposium on Electromagnetic Compatibility*, Denver, USA, 4–10 August 2013, pp. 551–556.
- ⁴¹L. Kraus, Z. Frait, and J. Schneider, *Phys. Status Solidi A* **64**, 449 (1981).
- ⁴²O. Acher and S. Dubourg, *Phys. Rev. B* **77**, 104440 (2008).
- ⁴³L. Levin, *Theory of Waveguides* (Newnes-Butterworth, London, 1975).
- ⁴⁴V. Myroshnychenko and C. Brosseau, *J. Appl. Phys.* **97**, 044101 (2005).
- ⁴⁵K. N. Rozanov, M. Y. Koledintseva, and J. L. Drewniak, *J. Magn. Magn. Mater.* **324**, 1063 (2012).
- ⁴⁶D. A. G. Bruggeman, *Ann. Phys.* **416**, 636 (1935).
- ⁴⁷D. J. Bergman, *Phys. Rep.* **43**, 377 (1978).
- ⁴⁸O. Wiener, "Die Theorie des Mischkörpers für das Feld der stationären Strömung," *Abh. Math.-Phys. Kl. Konigl. Sachh. Gesel. Wissen.* **32**, 509 (1912) [in German].
- ⁴⁹G. W. Milton, D. J. Eyre, and J. V. Mantese, *Phys. Rev. Lett.* **79**, 3062 (1997).